

Assay Principle for Modulators of Protein–Protein Interactions and Its Application to Non-ATP-Competitive Ligands Targeting Protein Kinase A

S. Adrian Saldanha,^{†,‡} Gregory Kaler,[‡] Howard B. Cottam,^{||} Ruben Abagyan,[‡] and Susan S. Taylor^{*,†,‡,⊥}

Department of Chemistry and Biochemistry, University of California, La Jolla, California 92093, Department of Molecular Biology, The Scripps Research Institute, 10550 North Torrey Pines Road, La Jolla, California 92037, Department of Medicine, University of California San Diego, La Jolla, California 92093; Moores Cancer Center, University of California at San Diego Medical Center, La Jolla, California 92093-0820, and Howard Hughes Medical Institute, University of California, La Jolla, California 92093

Targeting sites that modulate protein–protein interactions represents an ongoing challenge for drug discovery. We have devised an assay principle, named ligand-regulated competition (LiReC), in an effort to find non-ATP competitive small-molecule regulators for type I α cAMP-dependent Protein kinase (PKA-I α), a protein complex that is implicated in disease. Our assay based on the LiReC principle utilizes a competitive fluorescent peptide probe to assess the integrity of the PKA-I α complex upon introduction of an allosteric ligand. The developed fluorescence polarization method screens for small molecules that specifically protect (antagonists) or conversely activate (agonists) this protein complex. In high-throughput format, various cyclic nucleotide-derived agonists and antagonists are successfully detected with high precision. Furthermore, assay performance (Z' -factors above 0.7) far exceeds the minimum requirement for small-molecule screening. To identify compounds that operate through novel modes of action, our method shields the ATP-binding site and purposely excludes ATP-competitive ligands. These proof-of-principle experiments highlight the potential of the LiReC technique and suggest its application to other protein complexes, thereby providing a novel approach to identify and characterize modulators (small molecules, proteins, peptides, or nucleic acids) of protein–protein systems.

cAMP-Dependent Protein Kinase as a Drug Target. cAMP-dependent protein kinase (protein kinase A, PKA) is a ubiquitous serine/threonine protein kinase that phosphorylates intracellular protein substrates in response to the secondary messenger, adenosine 3',5'-cyclic monophosphate (cAMP). The PKA holoenzyme is composed of two catalytic (C) and two regulatory (R) subunits that form an inactive tetramer. Binding of four cAMP

molecules, two per R-subunit, activates PKA by causing the tetramer to dissociate into a dimer of R-subunits and two catalytically active C-subunits, thereby enabling phosphorylation of downstream PKA substrates. The R-subunit has two major roles. First, it maintains the C-subunit in an inactive state in the absence of cAMP, and second, it determines subcellular localization via specific interactions with A-kinase anchoring proteins (AKAPs). There are four isoforms of the PKA regulatory subunit (RI α , RI β , RII α , RII β) that diversify PKA-mediated signaling by differing in their abundance, affinity for the C-subunit, sensitivity to cAMP, and specificity for different AKAPs.^{1,2}

PKA is implicated in several cancers (e.g., carney complex,³ pituitary,⁴ and breast^{5,6}) and is also suggested to be a therapeutic target for diseases of the immune system (e.g., SLE and HIV).⁷ However, given the ubiquitous distribution of this protein kinase, it is unwise to target the ATP-binding site of the catalytic subunit, since an ATP-competitive inhibitor would just as likely kill healthy cells. Disease progression in some cancers correlates with abnormally high levels of the RI α isoform,^{5,6} and it is presumably the overabundance of type I α PKA holoenzyme (PKA-I α) that causes aberrant phosphorylation and promotes cancer. As a result, RI α antisense therapy is currently undergoing phase I/II clinical trials for the treatment of patients with malignant solid tumors.⁸ A small molecule that would selectively inhibit the catalytic action of PKA-I α (antagonist) may mimic the effect of RI α antisense

- (1) Feliciello, A.; Gottesman, M. E.; Avvedimento, E. V. *J. Mol. Biol.* **2001**, *308*, 99–114.
- (2) Skälhegg, B. S.; Tasken, K. *Front. Biosci.* **2000**, *5*, D678–693.
- (3) Casey, M.; Vaughan, C. J.; He, J.; Hatcher, C. J.; Winter, J. M.; Weremowicz, S.; Montgomery, K.; Kucherlapati, R.; Morton, C. C.; Basson, C. T. *J. Clin. Invest.* **2000**, *106*, R31–38.
- (4) Lania, A. G.; Mantovani, G.; Ferrero, S.; Pellegrini, C.; Bondioni, S.; Peverelli, E.; Braidotti, P.; Locatelli, M.; Zavanone, M. L.; Ferrante, E.; Bosari, S.; Beck-Peccoz, P.; Spada, A. *Cancer Res.* **2004**, *64*, 9193–9198.
- (5) Taimi, M.; Breitman, T. R.; Takahashi, N. *Arch. Biochem. Biophys.* **2001**, *392*, 137–144.
- (6) Miller, W. R. *Ann. N. Y. Acad. Sci.* **2002**, *968*, 37–48.
- (7) Skälhegg, B. S.; Funderud, A.; Henanger, H. H.; Hafte, T. T.; Larsen, A. C.; Kvissel, A. K.; Eikvar, S.; Orstavik, S. *Curr. Drug Targets* **2005**, *6*, 655–664.
- (8) Nesterova, M. V.; Cho-Chung, Y. S. *Clin. Cancer Res.* **2004**, *10*, 4568–4577.

* To whom correspondence should be addressed. E-mail: staylor@ucsd.edu.

[†] Department of Chemistry and Biochemistry, University of California.

[‡] The Scripps Research Institute.

[§] Department of Medicine, University of California San Diego.

^{||} Moores Cancer Center, University of California at San Diego Medical Center.

[⊥] Howard Hughes Medical Institute, University of California.

	A-site										B-site									
Consensus	I	:	V	.	-	S	F	G	E	L	A	L	P	R	A	A	:	:	-	
RI α _Human	I	V	V	A	T	S	F	G	E	L	A	L	P	R	A	A	V	D	W	
RI β _Human	I	V	V	V	T	S	F	G	E	L	A	L	P	R	A	A	V	E	W	
RII α _Human	I	I	V	V	G	S	F	G	E	L	A	L	P	R	A	A	I	E	S	
RII β _Human	I	I	V	V	G	S	F	G	E	L	A	L	P	R	A	A	I	E	S	

Figure 1. Alignment of residues that directly contact cAMP in the A and B sites for RI and RII isoforms. In the consensus, “:” and “.” denote strong and weak conservation (according to ClustalW convention) and “-” denotes no conservation. Residues separated by a space are nonadjacent in the protein sequence but come together in the 3D structure to form a discontinuous binding motif for cAMP. The A and B binding sites were identified by selecting all residues within a 3-Å radius of the cAMP mimic, Sp-cAMPS, bound to both sites in RI α from PDB: 1NE6.

therapy by repressing aberrant phosphorylation. In addition, a PKA-I α antagonist has been suggested as a therapeutic agent to improve T cell responsiveness to HIV.⁷ On the other hand, a small-molecule activator of PKA may also be of benefit. For example, S49 T-lymphoma cells undergo cAMP-stimulated apoptosis through activation of PKA.⁹

PKA Small-Molecule Ligands. Two classes of small-molecule modulators targeting PKA have been described. The first class represents ATP competitors that target the C-subunit and inhibit the catalytic function. However, potent ATP-competitive inhibitors of PKA, such as H89¹⁰ and staurosporine,¹¹ also inhibit other protein kinases as well as nonrelated cellular receptors,¹² thus compromising the therapeutic potential of this class of inhibitors. The second class comprises molecules related to the endogenous PKA regulator, cAMP.¹³ Cell-permeable derivatives have been designed that act as either agonists (activating the holoenzyme in the same way as cAMP) or antagonists (competing with cAMP for binding to the R-subunit but not inducing holoenzyme dissociation).

Targeting PKA Allosteric Sites. The cAMP-binding sites are obvious targets for novel non-ATP-competitive modulators of PKA function. To date, only cyclic nucleotide analogues have been reported to bind to these sites. However, as the charged cyclic phosphate group is a strict requirement, these compounds exhibit poor in vivo efficacy¹⁴ due to cell permeability and sensitivity to phosphodiesterases.

Crystal structures obtained for free R-subunit,¹⁵ complexes with cAMP analogues¹⁶ and most recently for R-subunit bound to the C-subunit¹⁷ bring insights into the allosteric mechanism behind cAMP binding and allow correlation between the sequence and structure of the cAMP-binding sites. The R-subunit is composed of two homologous domains, each having a high-affinity cAMP-binding site (named A and B sites). Sequence divergence of A

and B sites (Figure 1) suggests that small molecules can be discovered that distinguish between them. Indeed, synthetic cAMP analogues have been designed that bind preferentially to one or the other site.¹³ The most recent structure of a deletion mutant of type I α R-subunit (containing A domain only) reveals major conformational changes in the A site upon binding to C-subunit.¹⁷ This finding suggests that antagonists may be found that exploit the rearrangement of the A site between the holoenzyme (i.e., R–C complex) and free R-subunit.

Moreover, sequence divergence between the RI and RII isoforms is sufficient to suggest that selective binders may be designed. Figure 1 shows that 6 out of 19 residues directly in contact with cAMP in the A site and 11 out of 22 residues in the B site differ between RI and RII subtypes. The discovery of isoform-specific binders then opens up the possibility for selectively targeting only the disease-associated forms of PKA.

Limitations in High-Throughput Screening (HTS) of Protein Kinases. Assays commonly used in HTS against protein kinases follow substrate or ATP turnover as measured by a variety of approaches, including luminescence,¹⁸ fluorescent polymer superquenching,¹⁹ homogeneous time-resolved fluorescence,²⁰ scintillation proximity assay,²¹ AlphaScreen,²² electrophoretic shift,²³ and fluorescence polarization (FP).²⁴

The identification of non-ATP-competitive ligands that modulate kinase function through stabilizing active or inactive conformational states (e.g., allosteric modulators) would provide a novel mechanism of action for kinase drugs. In principle, existing kinase HTS assays can also identify these types of ligands as demonstrated by the discovery of allosteric Akt inhibitors.²⁵ In practice, however, discerning true non-ATP-competitive modulators from

(9) Zhang, L.; Insel, P. A. *J. Biol. Chem.* **2004**, *279*, 20858–20865.

(10) Chijiwa, T.; Mishima, A.; Hagiwara, M.; Sano, M.; Hayashi, K.; Inoue, T.; Naito, K.; Toshioka, T.; Hidaka, H. *J. Biol. Chem.* **1990**, *265*, 5267–5272.

(11) Matsumoto, H.; Sasaki, Y. *Biochem. Biophys. Res. Commun.* **1989**, *158*, 105–109.

(12) Son, Y. K.; Park, W. S.; Kim, S. J.; Earm, Y. E.; Kim, N.; Youm, J. B.; Warda, M.; Kim, E.; Han, J. *Biochem. Biophys. Res. Commun.* **2006**, *341*, 931–937.

(13) Schwede, F.; Maronde, E.; Genieser, H.; Jastorff, B. *Pharmacol. Ther.* **2000**, *87*, 199–226.

(14) Prinz, A.; Diskar, M.; Erlbruch, A.; Herberg, F. W. *Cell Signal* **2006**.

(15) Wu, J.; Brown, S.; Xuong, N. H.; Taylor, S. S. *Structure* **2004**, *12*, 1057–1065.

(16) Wu, J.; Jones, J. M.; Nguyen-Huu, X.; Ten, Eyck, L. F.; Taylor, S. S. *Biochemistry* **2004**, *43*, 6620–6629.

(17) Kim, C.; Xuong, N. H.; Taylor, S. S. *Science* **2005**, *307*, 690–696.

(18) Singh, P.; Lillywhite, B.; Bannaghan, C.; Broad, P. *Comb. Chem. High Throughput Screen* **2005**, *8*, 319–325.

(19) Xia, W.; Rininsland, F.; Wittenburg, S. K.; Shi, X.; Achyuthan, K. E.; McBranch, D. W.; Whitten, D. G. *Assay Drug Dev. Technol.* **2004**, *2*, 183–192.

(20) Beasley, J. R.; McCoy, P. M.; Walker, T. L.; Dunn, D. A. *Assay Drug Dev. Technol.* **2004**, *2*, 141–151.

(21) Mallari, R.; Swearingen, E.; Liu, W.; Ow, A.; Young, S. W.; Huang, S. G. *J. Biomol. Screen* **2003**, *8*, 198–204.

(22) Von, Leoprechting, A.; Kumpf, R.; Menzel, S.; Reulle, D.; Griebel, R.; Valler, M. J.; Buttner, F. H. *J. Biomol. Screen* **2004**, *9*, 719–725.

(23) Miick, S. M.; Jalali, S.; Dwyer, B. P.; Havens, J.; Thomas, D.; Jimenez, M. A.; Simpson, M. T.; Zile, B.; Huss, K. L.; Campbell, R. M. *J. Biomol. Screen* **2005**, *10*, 329–338.

(24) Sportsman, J. R.; Gaudet, E. A.; Boge, A. *Assay Drug Dev. Technol.* **2004**, *2*, 205–214.

(25) Barnett, S. F.; Defeo-Jones, D.; Fu, S.; Hancock, P. J.; Haskell, K. M.; Jones, R. E.; Kahana, J. A.; Kral, A. M.; Leander, K.; Lee, L. L.; Malinowski, J.; McAvoy, E. M.; Nahas, D. D.; Robinson, R. G.; Huber, H. E. *Biochem. J.* **2005**, *385*, 399–408.

ATP competitors, as well as promiscuous compounds that act through high-stoichiometry binding or by causing protein aggregation or denaturation, has not been rigorously pursued. Furthermore, a bias for ATP competitors is inherent in these screens because they are performed at relatively low ATP concentrations compared to the affinity for kinases (e.g., K_d for ATP binding to PKA is $\sim 25 \mu\text{M}$ ²⁶). This has undoubtedly resulted in all top-ranking HTS hits, and subsequently drug-leads, being ATP-competitive.

Our ultimate goal is to identify novel subtype-selective small-molecule modulators of PKA that mediate their effect through binding to sites distinct from the ATP-binding site. This report describes development of a novel assay, with fluorescence polarization as readout, designed to identify non-ATP-competitive small molecules targeting PKA-I α .

EXPERIMENTAL SECTION

Reagents. The PKA inhibitor peptide IP20 (Thr–Thr–Tyr–Ala–Asp–Phe–Ile–Ala–Ser–Gly–Arg–Thr–Gly–Arg–Arg–Asn–Ala–Ile–His–Asp) was synthesized at the University of California at San Diego (UCSD) in the Peptide and Oligonucleotide Core Facility and purified by HPLC. Succinimidyl esters of (5,6)-carboxyfluorescein (5,6-FAM) and Texas red-X were from Invitrogen (Carlsbad, CA). 8-Br-adenosine 3',5'-cyclic monophosphorothioate (Rp-8-Br-cAMPS) was from Axxora (San Diego, CA). cAMP, 2'-deoxyadenosine 3',5'-cyclic monophosphate (deoxy-cAMP), guanosine 3',5'-cyclic monophosphate (cGMP), and PKI(14–24) amide (Gly–Arg–Thr–Gly–Arg–Arg–Asn–Ala–Ile–His–Asp–NH₂) were from Aldrich (Milwaukee, WI). ATP-competitive inhibitors (H89 and staurosporine) were obtained from LC Laboratories (San Diego, CA) and 2-(3,5-*O*-phosphinico- β -D-ribofuranosyl)-4-thiazolecarboxamide (cTzMP) from the Developmental Therapeutics Program, National Cancer Institute.

Synthesis of Labeled IP20. IP20 was conjugated at the N-terminus with succinimidyl activated carboxyfluorescein (FAM-IP20) or Texas red-X (TR-IP20). To synthesize FAM-IP20, 1 mg of 5,6-FAM succinimidyl ester and 2 mg of IP20 were incubated in 1 mL of PBS/DMF (50:50) overnight at 4 °C with gentle agitation. The fluorescent peptide was purified by C18 reversed-phase HPLC with a water/acetonitrile gradient (0.08% TFA). FAM-IP20 eluted in 38% acetonitrile. To synthesize TR-IP20, 1 mg of Texas red-X succinimidyl ester and 2 mg of IP20 were incubated in 1 mL of PBS/DMF (20:80) overnight at 4 °C with gentle agitation. The fluorescent peptide was purified by C18 reversed-phase HPLC and eluted in 49% acetonitrile.

Protein Expression and Purification. To minimize reagent preparation for HTS, stable constructs for the C- and R-subunits were used, namely, the C199A mutant of the C-subunit, which can be stored at 4 °C for over 1 year, and the $\Delta 1$ –91 deletion mutant of type I α R-subunit, RI α ($\Delta 1$ –91), lacking the dimerization docking domain and thus less prone to aggregation. The C199A mutant and wildtype C-subunit showed identical binding profiles with FAM-IP20 (data not shown), while the binding and activation behavior of the deletion mutant is nearly identical to wildtype RI α .²⁷ The C199A mutant of recombinant murine catalytic sub-

unit²⁸ and bovine RI α ($\Delta 1$ –91)²⁹ were expressed and purified from *Escherichia coli* as previously described.

Fluorescence Polarization Readings. Fluorescence readings were taken on a GeniosPro microplate reader (Tecan, Research Triangle Park, NC) with solid black 96-well untreated Costar (Corning, Catalog No. 3915) or 384-well Fluotrac-200 plates (Greiner, Catalog No. 781076). Fluorescein FP readings were with 485-nm excitation (20-nm bandpass) and 535-nm emission (20-nm bandpass) filters, and the supplied 510-nm dichroic mirror. Texas red FP readings were with 570-nm excitation (20-nm bandpass) and 630-nm emission (30-nm bandpass) filters and a 590-nm dichroic mirror from Tecan.

FP values (P) were calculated in millipolarization units (mP),

$$P = 1000 \times \frac{I_{\parallel} - G \times I_{\perp}}{I_{\parallel} + G \times I_{\perp}}$$

where I_{\parallel} and I_{\perp} are the emission intensities recorded, respectively, in the parallel and perpendicular directions relative to the plane of excitation polarization, after background intensity correction. G -factor values (G) for the fluorescein and Texas red spectral windows were measured with 1 nM fluorescein and a red low polarization standard (P2889) from Invitrogen.

Catalytic Subunit Binding and Competition Experiments.

Unless specified otherwise, all concentration-dependent binding and competition experiments were performed using 2-fold dilution series in the assay buffer: 50 mM HEPES (pH 7.0), 0.005% Triton-X 100, 10 mM MgCl₂, 2 mM ATP, and 2 mM DTT. In a typical experiment, 12 different concentrations of a test compound or protein were tested in at least duplicate. FAM-IP20- and TR-IP20-binding experiments were performed by adding 5 μL of C-subunit in 50 mM HEPES (pH 7.0) to 45 μL of FAM-IP20 or TR-IP20 solution in the assay buffer. Final concentrations were as follows: 0.5–512 nM C-subunit and 1 or 50 nM FAM-IP20 or 40 nM TR-IP20. The ATP concentration dependence of IP20 binding was measured by varying ATP concentration (12.5 nM to 12.8 μM) in the assay buffer, with 1 nM FAM-IP20 and 5 nM C-subunit. Competition experiments with PKI(14–24) were performed at 156 nM to 100 μM PKI(14–24), 1 nM FAM-IP20 and 5 nM C-subunit in the assay buffer. A stable FP reading was reached within 30 min upon addition of all the reagents and remained constant for at least 16 h. Binding and displacement curves were fit using Prism 4 software (GraphPad, San Diego, CA).

Holoenzyme Binding and Competition Experiments.

PKA-I α was formed in situ by combining C-subunit with 1.2 molar excess of R-subunit in the assay buffer 5 min prior to performing the study. This period is sufficient to form a stable holoenzyme complex that is completely resistant to displacement by the fluorescent IP20 probe in the absence of an agonist. Typically, the FP reading was taken within 1 h of adding all the reagents. The concentration dependence for cyclic nucleotides was measured by adding 1 μL of cyclic nucleotide solution in DMSO to 49 μL of assay buffer containing 40 nM TR-IP20, 64 nM C- and 77 nM R-subunits. Final cyclic nucleotide concentrations were as

(26) Lew, J.; Coruh, N.; Tsigelny, I.; Garrod, S.; Taylor, S. S. *J. Biol. Chem.* **1997**, *272*, 1507–1513.

(27) Herberg, F. W.; Dostmann, W. R.; Zorn, M.; Davis, S. J.; Taylor, S. S. *Biochemistry* **1994**, *33*, 7485–7494.

(28) Gangal, M.; Cox, S.; Lew, J.; Clifford, T.; Garrod, S. M.; Aschbacher, M.; Taylor, S. S.; Johnson, D. A. *Biochemistry* **1998**, *37*, 13728–13735.

(29) Su, Y.; Dostmann, W. R.; Herberg, F. W.; Durick, K.; Xuong, N. H.; Ten, Eyck, L.; Taylor, S. S.; Varughese, K. I. *Science* **1995**, *269*, 807–813.

follows: 20 nM–20 μ M cAMP, 200 nM–200 μ M cGMP, 100 nM–100 μ M cTzMP, or 2 μ M–2 mM deoxy-cAMP.

High-Throughput Assay Format. HTS was performed by adding 1 μ L of a test compound solution in DMSO to 49 μ L of assay buffer containing TR-IP20, C-subunit, R-subunit, and cGMP. The final composition of the assay mixture was as follows: 25 μ M test compound (unless stated otherwise), 40 nM TR-IP20, 64 nM C-subunit, 77 nM R-subunit, and 3 μ M cGMP in the assay buffer with 2% DMSO. In the absence of test compound (negative control samples), a midrange FP value was registered corresponding to \sim 50% bound TR-IP20 fraction.

Each screening plate contained eight half-maximal response control wells (no test compound, just 1 μ L DMSO added and FP response due to 3 μ M cGMP), eight agonist control wells (500 μ M cGMP final, maximal FP reading), and eight antagonist control wells (50 μ M Rp-8-Br-cAMPS final, minimal FP reading). In addition, readings from four buffer blank wells were taken for the background intensity correction.

For both agonistic and antagonistic responses, Z' -factors were calculated by

$$Z'_{\text{agonist}} = 1 - \frac{3 \times (\text{SD}_{\text{agonist}} + \text{SD}_{1/2\text{max control}})}{|P_{\text{agonist}} - P_{1/2\text{max control}}|}$$

$$Z'_{\text{antagonist}} = 1 - \frac{3 \times (\text{SD}_{\text{antagonist}} + \text{SD}_{1/2\text{max control}})}{|P_{\text{antagonist}} - P_{1/2\text{max control}}|}$$

FP values (P) and standard deviation (SD) were determined for the agonist, antagonist, and half-maximal response control wells.

RESULTS AND DISCUSSION

Assay Design. An assay was required that is capable of detecting both PKA- α agonists (inducing holoenzyme dissociation) and antagonists (compounds that protect holoenzyme). Recently, AlphaScreen technology has been used for this purpose, with C- and R-subunits attached to donor and acceptor beads, respectively, so that formation of the PKA protein complex brings the beads into proximity and luminescence is emitted.³⁰

We chose to develop a new technique for probing the integrity of the PKA holoenzyme complex that does not require protein attachment or labeling. The developed assay is based on a new principle, ligand-regulated competition (LiReC) for probing protein–protein interactions. This technique utilizes a probe that competes with one of the protein partners for binding to the other protein partner. The concentration of the first protein partner is adjusted such that it outcompetes the probe and probe binding can only occur by introduction of a modulator that destabilizes the protein complex. Binding to a protein receptor may be measured by changes in fluorescence polarization³¹ if a small fluorescently labeled ligand is used as the probe.

To implement a LiReC assay for the PKA system, the binding partners are the C- and R-subunits, and the allosteric modulator will be a cyclic nucleotide. The heat-stable protein kinase inhibitors (PKIs) are a family of small proteins that inhibit PKA by binding to the substrate-binding site of the catalytic subunit with subna-

nomolar affinity.³² The high-affinity binding motif is found at residues 5–24, and the respective 20-mer peptide spanning this range (named PKI(5–24) or IP20) binds to the C-subunit with high affinity, with a K_i of 2.3 nM.³³ Thus, IP20 is the ideal probe for this novel method.

Our LiReC assay (Scheme 1) exploits the following facts: (i) IP20 and the R-subunit bind to overlapping sites on the catalytic subunit and thus compete with each other, and (ii) the R-subunit affinity for the C-subunit is cAMP-dependent. In the absence of cyclic nucleotide, the R-subunit affinity for the C-subunit (K_d of 0.39 nM²⁷) exceeds that of IP20 (K_i of 2.3 nM). However, binding of cyclic nucleotide to the R-subunit weakens the R–C complex and enables IP20 to bind to C-subunit. Consequently, fluorescently labeled IP20 can be used as a probe for the interaction of the C- and R-subunits.

Interaction of FAM-IP20 with the Catalytic Subunit.

Fluorescence polarization has been previously used to measure the binding of a fluorescently labeled variant of IP20 (labeled with fluorescein on a C-terminal cysteine) to the catalytic subunit of PKA, and a K_d of 31 nM was obtained.³⁴ A similar binding study was designed in which the N-terminus of IP20 was labeled with carboxyfluorescein (FAM-IP20) and the concentration dependence with catalytic subunit was measured (Figure 2a). A K_d of 4.4 nM and a Hill slope close to 1 was obtained in this experiment for the interaction of C-subunit with 1 nM FAM-IP20. This value is close to the K_i recorded for IP20 (2.3 nM) and demonstrates that N-terminal labeling does not significantly weaken IP20 binding.

We specifically aimed to use a high probe concentration, since this offers significant advantages in HTS assay format (see later). At a FAM-IP20 concentration of 50 nM (i.e., significantly above the K_d for the interaction with C-subunit), a steep concentration dependence was observed (Figure 2a). This pattern is consistent with quantitative titration of FAM-IP20 by C-subunit.

Published structural and biochemical studies show dramatic changes in the PKA conformation and in the affinity of the C-subunit for R-subunit or IP20 induced by ATP.²⁶ This behavior is synergistic, since in the presence of the R-subunit or IP20, the affinity of the C-subunit for ATP is also enhanced by over 3000-fold.²⁶ In agreement with these findings, the interaction between FAM-IP20 and C-subunit was sensitive to ATP concentration (Figure 2b). Therefore, to minimize possible interaction of test compounds with the ATP-binding site, all further experiments were performed at saturating concentrations of ATP (2 mM) and MgCl_2 (10 mM).

To prove probe specificity and demonstrate that this assay is not reporting artifacts such as protein or peptide aggregation, a truncated version of IP20, PKI(14–24), was shown to compete with FAM-IP20 for binding to C-subunit in a dose-dependent manner, with an IC_{50} of 2.7 μ M (Figure 2c).

Optimizing Assay Conditions for HTS. First, as mentioned previously, we wished to use the fluorescent probe at a high concentration, since this would improve assay performance by

(30) Gesellchen, F.; Prinz, A.; Zimmermann, B.; Herberg, F. W. *Eur. J. Cell Biol.* **2006**, *85*, 663–672.

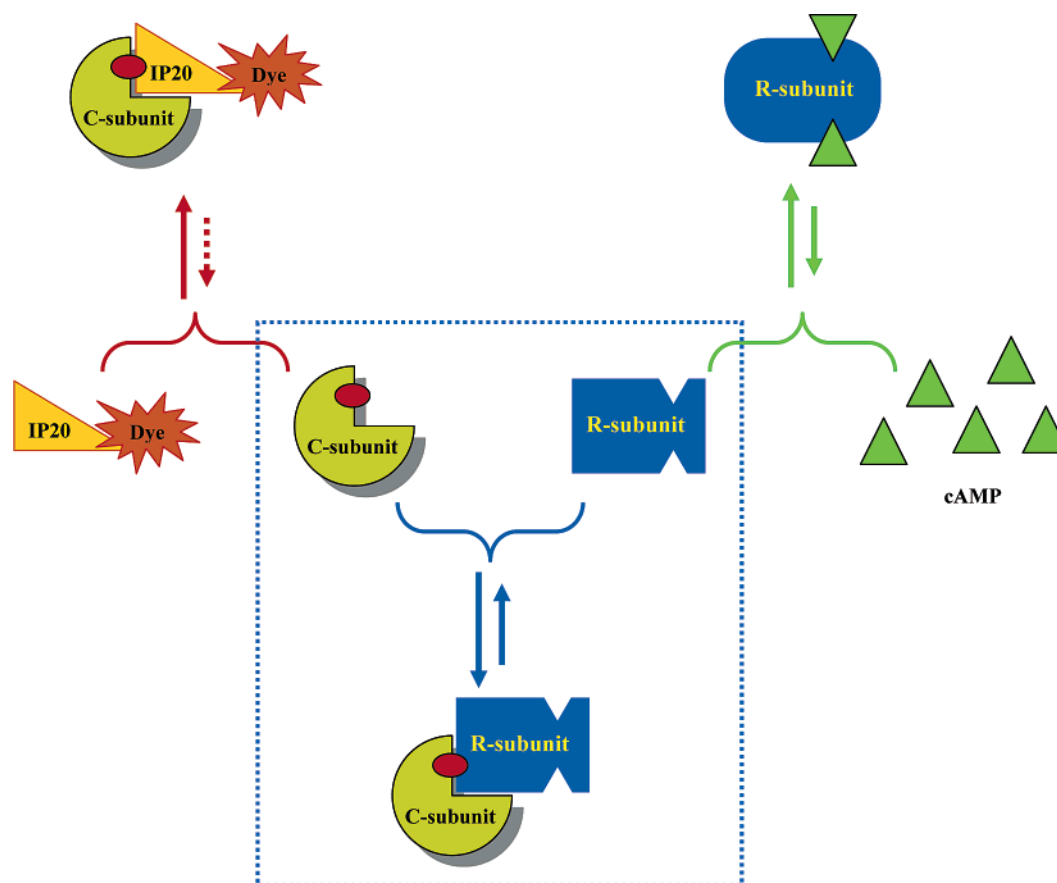
(31) Owicki, J. C. *J. Biomol. Screen* **2000**, *5*, 297–306.

(32) Scott, J. D.; Fischer, E. H.; Takio, K.; Demaille, J. G.; Krebs, E. G. *Proc. Natl. Acad. Sci. U.S.A.* **1985**, *82*, 5732–5736.

(33) Cheng, H. C.; Kemp, B. E.; Pearson, R. B.; Smith, A. J.; Misconi, L.; Van, Patten, S. M.; Walsh, D. A. *J. Biol. Chem.* **1986**, *261*, 989–992.

(34) Schneider, T. L.; Mathew, R. S.; Rice, K. P.; Tamaki, K.; Wood, J. L.; Schepartz, A. *Org. Lett.* **2005**, *7*, 1695–1698.

Scheme 1. LiReC Assay Principle As Applied to PKA^a



^a Binding of IP20 or R-subunit is mutually exclusive. In the absence of cyclic nucleotide (cAMP), R-subunit outcompetes IP20 and the R–C complex is the dominating species (blue box). However, cAMP binds to the R-subunit and weakens this complex, allowing IP20 to compete for C-subunit. Fluorescent labeling of IP20 enables the use of fluorescence polarization as a readout for peptide binding and consequently a probe for the integrity of the R–C complex. ATP/MgCl₂ (red oval) is necessary for high-affinity binding of either IP20 or R-subunit. A change in conformation between R- bound to C-subunit and free R is depicted by a change in shape. For simplicity, only the R–C half is depicted although PKA holoenzyme is a R₂C₂ complex.

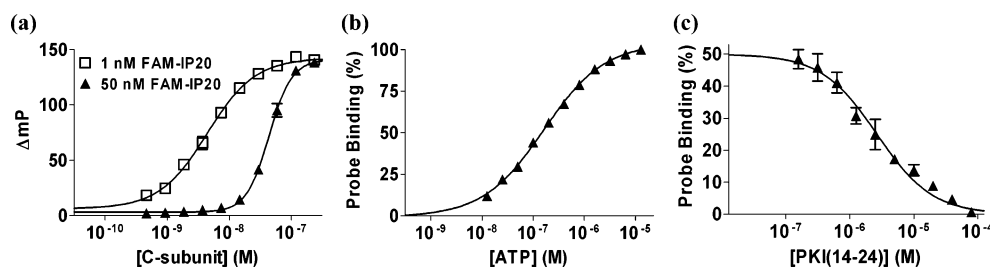


Figure 2. (a) Equilibrium binding studies between C199A C-subunit and FAM-IP20 at 1 or 50 nM. Experiments were performed with a twofold serial dilution series for C-subunit ($n = 4$) in a final volume of 50 μ L. The affinity for 1 nM FAM-IP20 was found by fitting to a sigmoidal dose response with $K_d = 4.4 \pm 0.2$ nM and Hill slope = 1. (b) Dependence on ATP concentration of FAM-IP20 binding to C-subunit. The experiment was performed using 1 nM FAM-IP20 and 5 nM C-subunit with a twofold serial dilution series for ATP ($n = 3$) in a final volume of 165 μ L. Fitting to a sigmoidal dose response gave $EC_{50} = 145 \pm 8$ nM, Hill slope = 1. (c) Displacement of FAM-IP20 from C-subunit by PKI(14–24). The experiment was performed at fixed concentrations of FAM-IP20 (1 nM) and C-subunit (5 nM) with a twofold serial dilution series for PKI(14–24.) in a final volume of 50 μ L ($n = 4$). Fitting to a sigmoidal dose response gave $IC_{50} = 2.7 \pm 0.3$ μ M and Hill slope = 1.

reducing optical interference from test compounds and thus eliminate a significant fraction of false hits during screening. In a regular competition binding assay, a probe concentration significantly exceeding the K_d for its interaction with the binding site would compromise screening, since weak competitors, which may become promising candidates through lead optimization, will be missed. However, this is not the case with our novel LiReC assay (Scheme 1), in which test compounds do not directly compete with the probe (fluorescently labeled IP20), but regulate the

affinity of another assay component (R-subunit) that competes with the probe for binding to a common target (C-subunit).

The use of red-shifted fluorescent dyes in FP small-molecule screening provides additional advantage, since compound interference is minimized at longer excitation and emission wavelengths.^{31,35} For this reason, IP20 was labeled at the N-terminus with a long-wavelength fluorescent dye, Texas red-X. The obtained

(35) Vedvik, K. L.; Eliason, H. C.; Hoffman, R. L.; Gibson, J. R.; Kupcho, K. R.; Somberg, R. L.; Vogel, K. W. *Assay Drug Dev. Technol.* **2004**, *2*, 193–203.

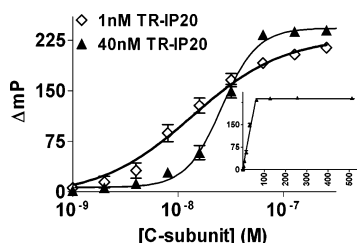


Figure 3. Equilibrium binding results between C199A C-subunit and TR-IP20 at 1 or 40 nM. A twofold serial dilution series for C-subunit ($n = 4$) in a final volume of 50 μL was used. The affinity for 1nM TR-IP20 was found by fitting to a sigmoidal dose response with $K_d = 19.4 \pm 0.7$ nM. Inset: The response with 40 nM TR-IP20 is plotted on a linear scale and shows quantitative titration.

fluorescent peptide, TR-IP20, at 1 nM showed 4-fold weaker binding (K_d of 19.4 nM; see Figure 3) to C-subunit compared to FAM-IP20, and again when used at a high concentration (40 nM), a steep concentration dependence was observed (Figure 3). The same data plotted on a linear concentration scale (Figure 3, inset) show a linear increase in the probe bound fraction followed by a plateau, which is indicative of quantitative titration. An added bonus by using TR-IP20 is a larger response window ($P_{\text{bound}} - P_{\text{free}}$) of 237 mP, compared to 136 mP for FAM-IP20. This may reflect a more restricted mobility upon binding of the Texas red moiety or to the longer fluorescence lifetime of Texas red (4.5 ns) compared to fluorescein (4.1 ns).³⁶

The following conditions were found optimal for assaying with TR-IP20: probe concentration of 40 nM, C-subunit concentration of 64 nM (close to the saturation of the FP response), and R-subunit concentration of 77 nM (a 1.2-fold molar excess over C-subunit was required to form holoenzyme when TR-IP20 is present). In this system, practically all of the C-subunit is in complex with the R-subunit, leaving TR-IP20 unbound (low FP readout).

To gauge the effectiveness of this system for probing the R–C interaction, the change in FP signal was measured at varying concentrations of four PKA agonists, namely, the cyclic nucleotides cAMP, deoxy-cAMP, cGMP and cTzMP (Figure 4). The potency of cAMP (EC_{50} of 59 nM) is consistent with literature values of less than 100 nM.^{37,38} A steep dose response observed for cAMP is a consequence of using R-subunit at a concentration that is significantly above the affinity for its interaction with cAMP (K_d of 1.7 nM³⁹). This rationale is in line with the more gradual response curves observed for the three other weaker binding cyclic nucleotides.

Although PKA responds endogenously to cAMP, previous findings that cGMP is a weaker activator of PKA- α were corroborated. Interestingly, activation by cTzMP (EC_{50} of 614 nM), which lacks the nucleobase core, is intermediate between cAMP (EC_{50} of 59 nM) and cGMP (EC_{50} of 3.12 μM). The 2'-deoxyribose derivative of cAMP was also tested and found to be a 1000-fold weaker activator (EC_{50} of 53.8 μM) than cAMP. This simple structure–activity series highlights the greater importance of the 2'-hydroxy on the ribose ring compared to the nucleobase.

High-Throughput Assay for Screening Both PKA Agonists and Antagonists. The described assay system involving fluorescent peptide (TR-IP20), C-subunit, and R-subunit is appropriate for the screening of PKA agonists. To broaden the scope and enable detection of both agonists and antagonists, a robust HTS format was designed incorporating a four-component system with TR-IP20, C- and R-subunits and cyclic nucleotide (Scheme 2). In this system, concentrations of C, R-subunit, and a cyclic nucleotide are adjusted such that about half of fluorescently labeled IP20 is bound to the catalytic subunit and the other half is free. As a result, a half-maximal FP signal is observed that is proportional to the bound fraction of the probe. Given the steep concentration dependence of cAMP-induced activation (Figure 4) and to offer a better screen-to-screen reproducibility, a weaker agonist, cGMP was used at a concentration equal to its EC_{50} of 3 μM . Agonists are compounds that weaken the R–C complex allowing more TR-IP20 to bind to C-subunit. This results in an increase of the bound probe fraction and, as a consequence, an increase in the FP value. In contrast, an antagonist is a compound that shields the R–C complex. Consequently, more C-subunit will form a stable complex with R-subunit, and less will be available to bind TR-IP20, so that the fraction of bound probe will be reduced and the FP signal will decrease.

LiReC Assay Performance in HTS Format. To assess the performance of our LiReC assay in HTS format, the Z' -factor, a statistical parameter that considers both the response magnitude and variation,⁴⁰ was calculated. An assay was performed in a 384-well plate with half-maximal response control wells (3 μM cGMP), agonist control wells (500 μM cGMP), and antagonist control wells (3 μM cGMP and 50 μM Rp-8-Br-cAMPS). Values obtained, for Z'_{agonist} of 0.75 and $Z'_{\text{antagonist}}$ of 0.77, far exceed the minimum requirement of 0.5 for high-throughput screening⁴⁰ and demonstrate the robustness of this assay.

Next, a real screen was conducted on an in-house compound collection, all tested at 25 μM (three sets totaling 134 compounds, Figure 5a). Our collection consisted of a structurally diverse set of heterocycles (mainly purine and xanthine analogues) and purine-like ribonucleosides. Several of the nucleosides were naturally occurring antibiotics (e.g., tubercidin, toyokamycin, sangivamycin, formycin A, minimycin, and pyrazomycin). Z' -Factors were consistently over 0.73 when these compounds were screened. Included in set 1 are the known PKA modulators 8-Cl-cAMP (agonist) and Rp-8-Br-cAMPS (antagonist).

Finally, The designed assay has demonstrated its ability not only to identify antagonists but also to accurately quantify their potencies. Thus, based on the concentration–response dependence for Rp-8-Br-cAMPS (Figure 5b), the IC_{50} value of 617 nM was calculated.

Resistance to ATP Competitors. It may be suspected that ATP competitors will register as antagonists, since they will displace ATP from its binding site, leading to a decrease in the IP20 probe affinity for C-subunit (Figure 3), so that less of the probe is bound and thus a lower FP signal is recorded. However, it has been shown that the affinity of ATP in the presence of IP20 improves by over 3000-fold (i.e., 25 μM to 7.3 nM²⁶). A positive

(36) Zhang, R.; Mayhoad, T.; Lipari, P.; Wang, Y.; Durkin, J.; Syto, R.; Gesell, J.; McNemar, C.; Windsor, W. *Anal. Biochem.* **2004**, *331*, 138–146.

(37) Cadd, G. G.; Uhler, M. D.; McKnight, G. S. *J. Biol. Chem.* **1990**, *265*, 19502–19506.

(38) Shabb, J. B.; Ng, L.; Corbin, J. D. *J. Biol. Chem.* **1990**, *265*, 16031–16034.

(39) Dostmann, W. R.; Taylor, S. S.; Genieser, H. G.; Jastorff, B.; Døskeland, S. O.; Olgred, D. *J. Biol. Chem.* **1990**, *265*, 10484–10491.

(40) Zhang, J. H.; Chung, T. D.; Oldenburg, K. R. *J. Biomol. Screen* **1999**, *4*, 67–73.

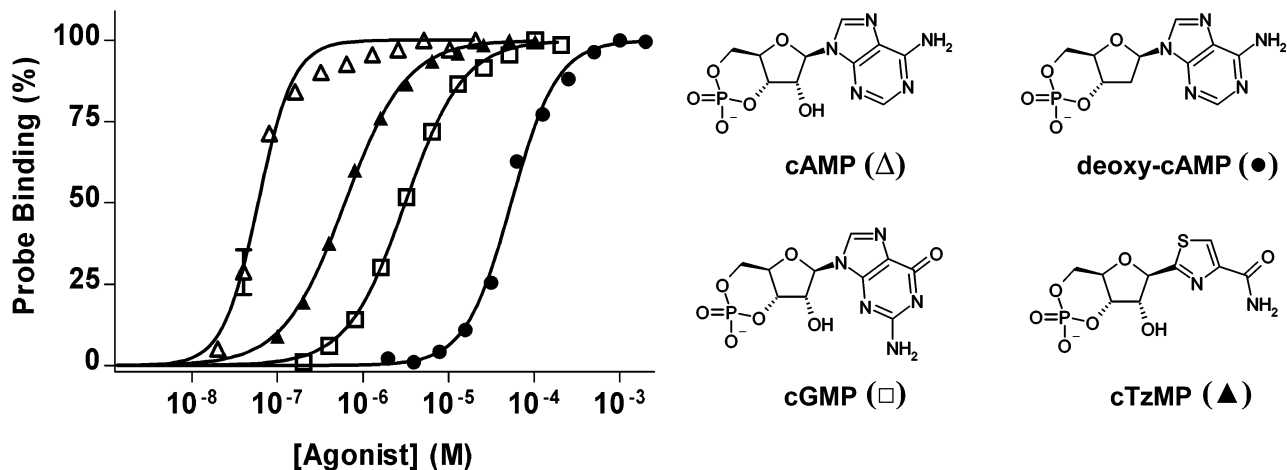
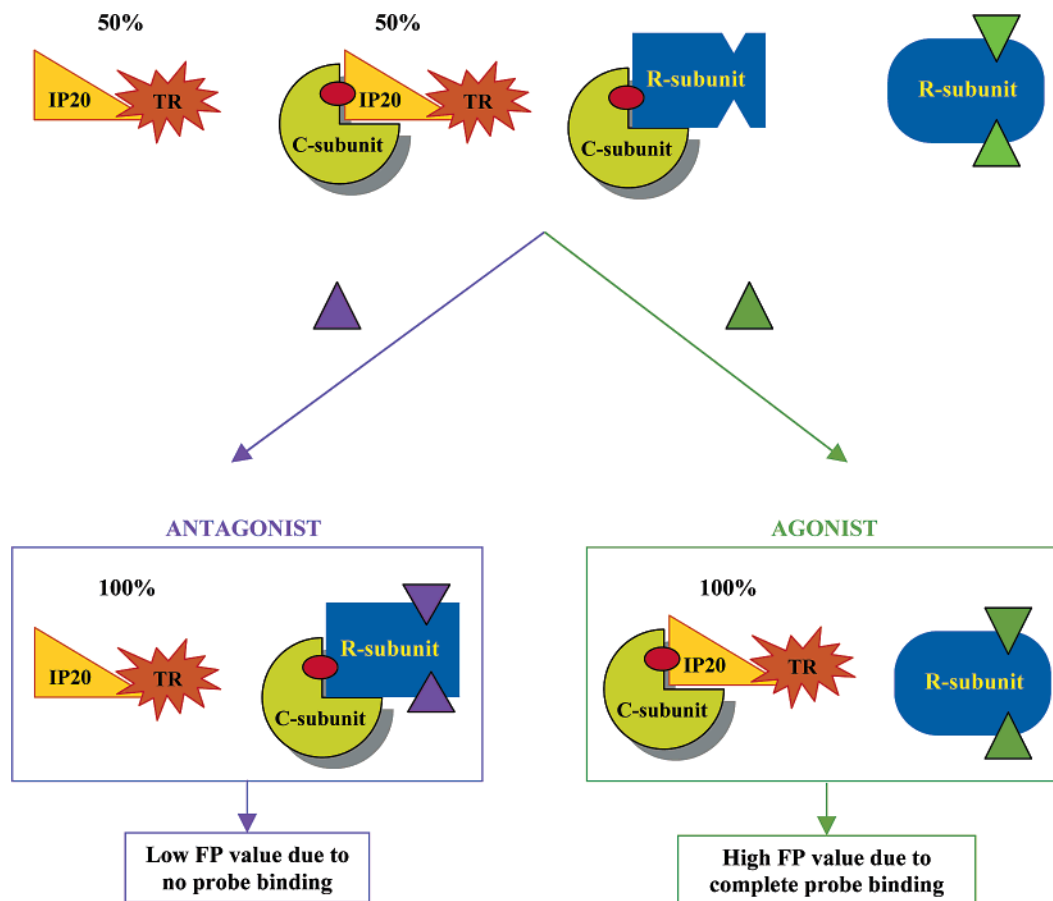


Figure 4. Activation by cAMP (Δ), cTzMP (▲), cGMP (□), and deoxy-cAMP (●). With fixed concentrations of TR-IP20 (40 nM), C-subunit (64 nM), and R-subunit (77 nM) and with $n = 2$. Dose responses were fit to sigmoidal behavior with a variable slope. cAMP ($EC_{50} = 59 \pm 3$ nM, Hill slope = 2.1), cTzMP ($EC_{50} = 614 \pm 13$ nM, Hill slope = 1.3), cGMP ($EC_{50} = 3.12 \pm 0.06$ μ M, Hill slope = 1.2), and deoxy-cAMP ($EC_{50} = 53.8 \pm 1.9$ μ M, Hill slope = 1.6). Structures of the cyclic nucleotide agonists are shown.

Scheme 2. LiReC Assay in HTS Format^a



^a A C199A mutant of C-subunit and a R1α(Δ1–91) truncation of R-subunit are used. This R-subunit construct cannot dimerize but otherwise is almost identical to wildtype. An agonist (▲) at its EC_{50} concentration will allow 50% of TR-IP20 to bind, eliciting a half-maximal FP response. Another agonist (▲) will further weaken the R–C complex, allowing more TR-IP20 to bind and increasing the FP signal. Alternately, an antagonist (▲) competes with agonist and shields the R–C complex, preventing binding of TR-IP20 to C-subunit and decreasing the FP signal.

consequence of this behavior is that with the high ATP concentration (2 mM) in the assay it is unlikely that ATP competitors will appear as hits. As proof, no reduction in FP signal was observed with the potent ATP competitors, H89 (K_i of 49 nM¹⁰) and staurosporine (K_i of 7 nM¹¹), tested at 200 μ M (data not shown).

CONCLUSIONS

In the present study, a novel assay principle has been devised, ligand-regulated competition, that utilizes a competitive probe for a protein–protein binding site to identify and characterize modulators of protein–protein interactions. For the proof-of-principle

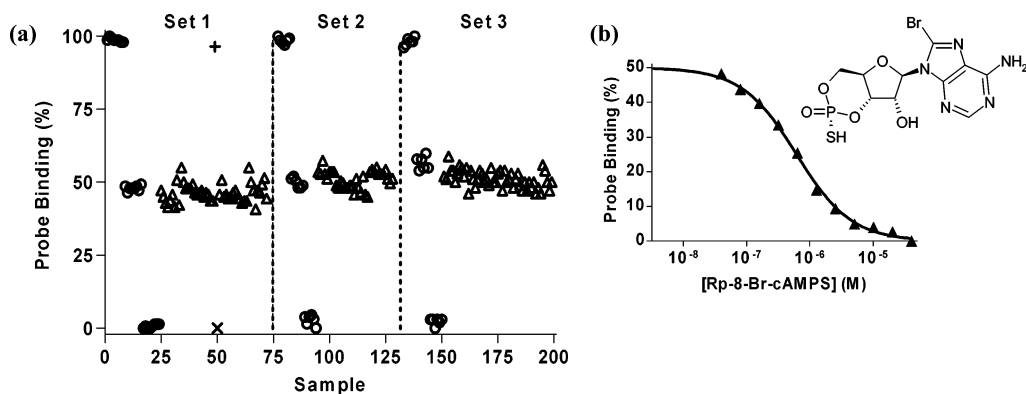


Figure 5. Screening results for 134 in-house compounds (Δ). Included in each screening set were 8 agonist response (500 μ M cGMP), 8 half-maximal, and 8 antagonist response (50 μ M Rp-8-Br-cAMPS) controls (all shown as \circ). Z -Factors for each screen were calculated from these controls: set 1, $Z'_{\text{agonist}} = 0.91$, $Z_{\text{antagonist}} = 0.90$; set 2, $Z_{\text{agonist}} = 0.73$, $Z_{\text{antagonist}} = 0.81$; and set 3, $Z_{\text{agonist}} = 0.83$, $Z_{\text{antagonist}} = 0.78$. A compound is recognized as an agonist if the FP reading is significantly increased compared to the half-maximal control response but equal to or lower than the agonist control response or an antagonist if the FP reading is significantly decreased compared to the half-maximal control response but greater than or equal to the antagonist control response. An agonist, 8-Cl-cAMP (+), and an antagonist, Rp-8-Br-cAMPS (\times), were included in set 1. (b) Antagonism by Rp-8-Br-cAMPS. The competition experiment was performed with a twofold serial dilution series for Rp-8-Br-cAMPS ($n = 2$) and with fixed concentrations of TR-IP20 (40 nM), C-subunit (64 nM), R-subunit (77 nM), and cGMP (3 μ M) in a final volume of 50 μ L. The IC_{50} was determined with a sigmoidal dose response with $IC_{50} = 617 \pm 22$ nM and Hill slope = 1. The structure of Rp-8-Br-cAMPS is shown.

experiments, we chose the disease-relevant PKA-I α system, where the integrity of the catalytically inactive protein complex is sensitive to cyclic nucleotides. The next step will be to adapt this assay for other R-subunit subtypes (RI β , RII α , RII β) in order to find selective druglike small molecules for potential therapeutic benefit.

The described assay is superior to existing methods for high-throughput identification of novel druglike PKA regulators. A key advantage is shielding the ATP binding site so as not to be swamped with compounds that bind to this site. In addition, a format for the assay is described that can identify both agonists and antagonists even though they have opposing effects. We are now in a position to screen large libraries for novel compounds that modulate PKA function in an ATP independent manner.

Application to Other Protein–Protein Systems. We envision that ligand regulated competition can be applied to other systems where the stability of a protein complex is regulated by a modulator (i.e., proteins, peptides, small molecules, or nucleic

acids). Regulation by this modulator may occur through stabilization of the protein complex by formation of a ternary complex, destabilization through direct competition, or destabilization through allosteric selection of an alternate conformational state. All three mechanisms may be characterized with an appropriately designed LiReC assay.

ACKNOWLEDGMENT

This work is supported by NIH grants GM 19301 and GM 34921 to S.S.T. and a California Breast Cancer Research Program Postdoctoral Award to S.A.S.. We thank Mike Deal, Sventja von Daake, and Cecilia Cheng for preparing protein constructs.

Received for review June 17, 2006. Accepted September 29, 2006.

AC061104G